AD-A172 310   ACOUSTIC PROPAGATION USING COMPUTATIONAL FLUID DYNAMICS   1/1
                  (U) ARMY AVIATION SYSTEMS COMMAND ST LOUIS MO
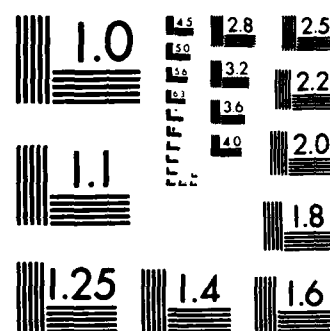   J D BAEDER ET AL.   JUN 86

UNCLASSIFIED   F/G 20/1   NL

ACOUSTIC PROPAGATION
USING COMPUTATIONAL FLUID DYNAMICS

J. D. Baeder, W. J. McCroskey, and G. R. Srinivasan[†]

U.S. Army Aeroflightdynamics Directorate - AVSCOM
NASA Ames Research Center, Moffett Field, California

[†]JAI Associates Inc., Mountain View, California

DTIC
ELECTE
SEP 2 3 1986
A

PAPER NO. _____

86 9 22 104

ACOUSTIC PROPAGATION
USING COMPUTATIONAL FLUID DYNAMICS

J. D. Baeder
Research Scientist
and
W. J. McCroskey
Senior Staff Scientist
U.S. Army Aeroflightdynamics Directorate - AVSCOM
NASA Ames Research Center, Moffett Field, California
and
G. R. Srinivasan
Senior Research Scientist
JAI Associates Inc., Mountain View, California

Abstract

The propagation characteristics of several helicopter airfoil profiles have been investigated using the transonic small disturbance equation. A test case was performed to generate a moving shock that propagated off the airfoil. Various grids were then examined to determine their ability to accurately capture these propagating shock waves. Finally, the case of airfoil/vortex interactions was thoroughly studied over a wide range of Mach numbers and airfoil shapes with particular emphasis on the transonic regime; this results in a highly complicated fluctuation of lift, drag, and pitching moment. The calculated acoustic intensity levels, along with the details of the computational flow field, provide new insights into the understanding of transonic airfoil/vortex interactions.

Notation

a	=	speed of Sound
C	=	chord length
C_2	=	$-\frac{1}{2}(\gamma+1)M_\infty^2$
C_3	=	$-(\gamma-1)M_\infty^2$
C_L	=	lift coefficient
C_M	=	pitching moment coefficient
C_p	=	coefficient of pressure
C_{p_i}	=	initial coefficient of pressure
dB	=	acoustic intensity in decibels
$d\vec{r}$	=	incremental position vector
M_∞	=	free stream mach number
$\vec{q}$	=	nondimensional velocity
$\vec{q}_v$	=	nondimensional velocity induced by vortex
R	=	nondimensional distance to source in acoustic frame
R_1	=	nondimensional distance to source in computational frame
u,v	=	nondimensional velocities in the x- and y- directions, respecively
u_v,v_v	=	nondimensional velocities induced by the vortex
U_∞	=	freestream velocity
X,Y	=	directional coordinates
x,y	=	nondimensional directional coordinates
x_v,y_v	=	nondimensional vortex location
β^2	=	$1-M_\infty^2$
Γ_v	=	nondimensional vortex strength
Λ_i	=	intersection angle
ϕ	=	velocity potential
θ	=	angle downward from source in acoustic frame
θ_1	=	angle downward from source in computational frame

Introduction

The transonic flow phenomena that occur on the advancing blade tips of modern helicopters have major effects on the aerodynamic performance, vibratory loads, and acoustic radiation of the rotor. One of the primary influences on the advancing blade is the blade-vortex interaction, as shown in Fig. 1, which can result in large fluctuations in the lift, pitching moment, and drag with a corresponding propagation to the far field. As the intersection angle between the blade and the vortex ap-

proaches zero, the problem can be modeled in two dimensions; namely, as a concentrated vortex convecting past a stationary airfoil.

A variety of computational procedures for calculating the unsteady interaction of a helicopter rotor blade with a Lamb-like vortex of finite viscous core in subsonic and transonic flows have been developed for the limiting case of a two-dimensional parallel blade-vortex interaction [1-4]. Heretofore, most of these computations have been primarily concerned with the changing airloads and have neglected to look at the resulting propagated waves.

From Fig. 2, it can be seen that the fluctuation in pressure on the airfoil due to the vortex-interaction is at least an order of magnitude larger than that in front of the airfoil. Most computational meshes have been chosen to enhance the accuracy of the airloads by concentrating points near the airfoil, while failing to have adequate resolution off of the airfoil to capture propagating waves. Indeed, even in studies that looked off of the airfoil (along rays), little attention has been placed on adequate resolution of the far field regions. Without adequate resolution the results obtained might be misleading, especially if one does not examine the whole field of calculation.

On the other hand, most acoustic investigations of blade-vortex interactions have tended to use relatively simple aerodynamic theories to predict surface forces combined with linear acoustics to predict the far field acoustics. However, the Computational Fluid Dynamic (CFD) codes mentioned above can be utilized to extend the predictions of acoustic propagation to more complicated, highly non-linear flow regimes.

The rapid calculation of unsteady problems with a large number of grid points was possible since a small disturbance code (ATRAN2) was used. In addition, this code has been carefully validated in comparison with Euler and Navier-Stokes results [4]. By examining the far field regions one can see the effect of the grid on the resolution of the propagation of acoustic and other waves. One can then use the code in helping to evaluate airfoils at various flight conditions for their acoustic propagation.

Description of the Numerical Method

The computer code ATRAN2 developed at NASA Ames Research Center solves the two-dimensional transonic small disturbance equation. The highlights of the method are described below, while the details of the implementation have been previously described elsewhere [5-6].

Governing Equations and Solution Procedures

The transonic small disturbance equation assumes a thin airfoil in an inviscid, isentropic fluid. The combination of unsteady flow and a concentrated potential (irrotational) vortex disturbance requires some special attention if potential flow concepts are to be retained. The continuity and momentum equation can still be combined to give

$$\frac{\partial Q}{\partial t} + 2u\frac{\partial u}{\partial t} + (a^2 - u^2)\frac{\partial u}{\partial x} + a^2\frac{\partial v}{\partial y} = 0$$

where

$$Q = \int \left(\frac{\partial \vec{q}}{\partial t} - \vec{q} \times \nabla \vec{q}\right) \cdot d\vec{r} - f(t),$$

The flow field is solved by the prescribed-vortex, or perturbation, method. By analogy to shock-fitting this has also been called vortex fitting. The total velocity is thus decomposed into the following quantities: 1) the uniform free stream, $\vec{U}_\infty$; 2) the prescribed disturbance field, $\vec{q}_v$; and 3) an irrotational perturbation velocity field $\nabla\phi$ produced by the airfoil in the presence of the concentrated vortex. That is,

$$\vec{q} = \vec{U}_\infty + \vec{q}_v + \nabla\phi$$

Note that this decomposition of the velocity does not imply linearity. Both the boundary conditions and the governing equation for the airfoil disturbance potential, $\nabla\phi$, are altered by the introduction of $\vec{q}_v$, and independent solutions are not superposable for transonic flows.

The modified form of the unsteady transonic small disturbance equation is then given by

$$M_\infty^2 \phi_{tt} + 2M_\infty^2 \phi_{xt} =$$

$$\frac{\partial}{\partial x}[(\beta^2 + C_2\phi_x + C_3\phi_t)(\phi_x + u_v) - \beta^2 u_v] + \phi_{yy}$$

The boundary condition on the airfoil now becomes

$$\phi_y(x, y \to 0) = y_x + y_t - v_v$$

and the pressure coefficient remains

$$C_p = -2(\phi_x + \phi_t)$$

Computational Gridding

The first step in investigating the propagation of waves to the far field required determining the appropriate grid spacing and grid smoothness. Previous calculations concentrated points on the airfoil in order to accurately capture the shock wave and determine the resulting airloads. The grid was then stretched exponentially to the outer boundary.

It was found that a large number of points were also needed off the airfoil, in the mid field, in order to properly capture the propagating wave. In addition, if the grid spacing was not smooth the waves were distorted, reflected, or annihilated. Increasing the number of mesh points correspondingly increases the computer time and

therefore a compromise must be reached. For all the calculations in this paper it was found that a mesh consisting of 399 points in the x-direction and 195 points in the y-direction was suitable . This resulted in a computational time on the order of 300 seconds on the Cray-XMP for 30 chords of travel by the vortex. Every fifth point of the near field and mid field of the grid is shown in Fig. 3. Note that the regions directly in front of and behind the airfoil have a constant spacing of 0.03 chords in order to capture the propagating waves.

Frames of Reference

It is important to realize the different frames of reference that are used in CFD and Acoustics as shown in Fig. 4. In CFD the calculations are performed in a refere. ce frame fixed with respect to the airfoil (CFD frame). Consequently, in CFD the unsteady fluctuations in pressure are usually viewed in this reference frame. However, in acoustics one is usually interested in the unsteady fluctuations that a stationary observer would observe as the airfoil passes by (Acoustic frame).

In unsteady airfoil-vortex interactions the source of the propagated waves is primarily due to the large pressure fluctuations that occur near the leading edge when the vortex passes immediately underneath the leading edge. In transonic cases the movement of the shock also contributes to large pressure fluctuations on the airfoil surface. The transformation from the CFD frame of reference to the Acoustic frame of reference can therefore be accomplished by placing the observer a fixed distance from the source of propagation, which in the CFD frame convects with the observer at the free stream velocity.

Acoustic Theory

The two-dimensional transonic small disturbance equation used to calculate the interaction flow field of the airfoil-vortex interaction will capture a two-dimensional propagated wave. In order to understand the acoustic interpretation of this calculated propagation it is important to realize the differences between two-dimensional and three-dimensional acoustics as shown in Fig. 5.

First of all, in three-dimensions the acoustic wave from a point source in a stationary fluid will propagate with equal speed in all radial directions. For a point source in a moving fluid the speed of the upstream propagation will be less than that in the downstream direction. This motion will result in more energy being propagated upstream. In addition, in three-dimensions the shape of the waveform remains unchanged as it propagates. In two-dimensions the analogous situation is a line source. In this case, there will also be more energy directed upstream than downstream, when the line source is placed in a moving fluid. However, the waveform shape will not remain sharp as in the three-dimensional case. Rather, the waveform will tend to smear. This is due to the

fact that the propagation from different parts of the line source will take different times to reach the same point in the flowfield. Thus, although the initial waveform may be sharp, as the wave propagates it will tend to smear out, with a sharp beginning pulse followed by a smeared tail.

Secondly, in three-dimensions acoustic theory predicts that the far field disturbance amplitude should be inversely proportional to the distance from the source. In two-dimensions the far field pressure amplitude should be inversely proportional to the square root of the distance from the source.

Thirdly, when one examines the pressure time history of several points along a ray, one will notice that the amplitude of the fluctuating pressure does not scale exactly with the inverse of the square root of the distance from the source of propagation, especially in the near field as shown in Fig. 6a. The reason for this occurring can be understood by examining the pressure time history that a stationary observer would observe as an airfoil passes by, with no vortex present. In this case, the amplitude of the fluctuating pressure, as shown in Fig. 6b, falls off much more rapidly than that due to an acoustic source. Indeed, in the absence of any shock there should be no propagation to the far field. Thus, the initial pressure field should be subtracted off in order to better observe the acoustic effects of the vortex passing by the airfoil. When this is performed, as shown in Fig. 6c, the amplitude of this disturbance pressure scales very well with the inverse of the square root of the distance to the source.

Fourthly, in the far field the acoustic intensity can be approximated by taking the integral of the square of the disturbance pressure. In two-dimensions the acoustic intensity should therefore scale with the inverse of the distance to the source.

Results and Discussion

Numerical results for a variety of unsteady flow fields have been examined. The main purpose of this investigation was to study the propagation of waves in a transonic blade-vortex interaction. However, this is a rather complex interaction with large variations in lift, pitching moment, and drag. Therefore, simpler flow fields were also examined in order to better understand the vortex interactions.

The unsteady changes in the flowfield properties due to the passage of the vortex are of the same order as the steady flow properties that result in the absence of the vortex. For this reason and because of acoustic theory it is easier to visualize the propagating waves if the initial properties are subtracted, leaving the disturbance pressure. Also, as stated above, two-dimensional acoustic theory states that the far field pressure amplitude remains constant when scaled by the square root of the distance of the point from the source. For the case of blade-vortex interactions the position of the source cor-

responds approximately to the position of the vortex.

The acoustic results presented are all along a forty-five degree downward from the acoustic source. This is due to the fact that experiments show that the strongest propagation occurs along a thirty to forty-five degree ray downward from the vortex[7].

Symmetrically Thickening-Thinning Airfoil

In order to study the propagation of shock waves off of the front of an airfoil, a thickening-thinning, non-lifting NACA 0012 airfoil has been studied in both sub- and super-critical conditions. By studying both the sub- and super-critical cases one can separate the effects of a thickening-thinning airfoil alone, from the case of one with a moving shock wave. In Fig. 7 (super-critical case) the moving shock is shown to be well captured and moves off the front of the airfoil into the mid field. This would seem to be a classic case of Type-C motion as described by Tiedjman [8]. This also demonstrates the ability of the grid system and numerical formulation to capture and preserve a propagating shock wave. Note that when coarser meshes were used the propagating disturbance would smear as it left the vicinity of the airfoil.

Transonic Airfoil-Vortex Interaction

Airfoil-vortex interactions have been studied in order to investigate some of the parameters which affect the propagation of disturbances on the airfoil to the far field regions. Fig. 8 shows the initial pressure distribution on the airfoil, as well as four succesive positions of the vortex. In addition, the time history of the lift and pitching moment coefficients are plotted. This has been the traditional means of displaying airfoil-vortex interactions [1-4]. When one looks at successive contour plots of the pressure field in Fig. 9, one can better observe the interaction of the vortex with the airfoil and resulting shock system. Note that in this case the vortex passes through the shock wave ($x_v = 0.5$) and a bifurcation of the shock occurs ($x_v = 1.0$). In addition, the curvature of the shock changes as the vortex passes by. Such phenomena was first observed in calculations performed by Srinivasan, et al [4]. Although, there are hints of a propagating wave, they are not clearly visible due to the difference in order of magnitude between the steady and disturbance pressures in the vicinity of the airfoil.

The propagating wave and its structure is clearly visible though when one looks at Fig. 10 at the disturbance pressure caused by the airfoil-vortex interaction. Note how clearly the propagating wave stands out, even when viewed from such a large distance. It is also clearly visible that for this particular case much more energy is propagated in the upstream direction. In addition, the upper part of the wave is a compression-expansion-compression wave while the lower part of the wave is an expansion-compression-expansion wave, as expected.

The lower part of the wave's structure is highly complicated, since as the shock wave moves forward, a discontinuity seperates from the shock wave and propagates forward away from the airfoil. This discontinuity also weakens rapidly as it moves away from the airfoil.

Airfoil-Vortex Interaction Mach Number Effects

Airfoil-vortex interactions were examined over a wide range of mach numbers in order to better understand the resulting propagations. The disturbance pressure contours, as shown in Fig. 11, and the acoustic intensities, as shown in Figs. 12-13, were examined. From the disturbance pressure contours one can visualize some of the effects of compressibility, especially when nonlinear terms become important. At the low mach numbers the acoustic wave seems to be fairly symmetrical front and back, with only a slight preference for more acoustical energy to propagate forward. The acoustic wave is also almost exactly anti-symmetrical top and bottom, with a compression-expansion-compression wave on the top and an expansion-compression-expansion wave on the bottom. As the mach number increases a larger protion of the acoustic energy is propagated in the upstream direction. In addition, nonlinear effects, more pronounced on the bottom, tend to make the wave appear less anti-symmetric top and bottom. Especially note how in the transonic cases the presence of the shock on the bottom surface causes a much sharper discontinuity to propagate forward. It is also important to note that the amplitude of the pressure disturbance of the acoustic wave also increases with mach number as will be quantitatively demonstrated by calculating the acoustic intensities.

Fig. 12 plots the acoustic intensity versus distance for a ray 45 degrees down from the forward direction. For the subsonic cases the acoustic intensity is seen to vary with the inverse of the distance to the source as is predicted by two-dimensional acoustics. It would thus appear that nonlinear effects are small, as expected, and that the near field does not extend very far. The nonlinear transonic case demonstrates that the near field region extends farther out and even at ten chords the acoustic intensity does not vary according to linear two-dimensional acoustic theory. Fig. 13 is a polar plot of the acoustic intensity and helps to quantify some of the results shown qualitatively in the disturbance pressure contours. Especially note how in the nonlinear transonic case the results are no longer symmetric top and bottom. Fig. 14 is a plot of the acoustic intensity versus mach number and the results for the NACA 0012 airfoil (solid line) confirm the idea that the strength of the propagating wave will vary with the sixth power of the mach number. It also appears that in the nonlinear transonic regime this law no longer holds but instead it seems to vary with a smaller power of the mach number.

4

Airfoil-Vortex Interaction Airfoil Effects

It might be thought that the airfoil shape would have a drastic effect on the propagating wave. Therefore, besides the NACA 0012 airfoil, the 64A006 and SC1095 airfoils were studied over a wide mach number range. The resulting acoustic intensity levels are plotted in Fig. 14. From this figure it can be seen that in the linear regime, the airfoil shape has little or no effect on the acoustic intensity of the resulting propagation. It thus appears that in this mach number range the acoustic intensity is only affected by the strength of the vortex and the vertical displacement between the airfoil and vortex, not the airfoil shape. However, there are slight differences when one reaches mach numbers such that nonlinear compressibility effects become important (shocks). To the extent that airfoil shape influences the formation and decay of these shocks, the airfoil shape does influence the resulting propagation.

Summary and Conclusions

A series of computed airloads and flow fields have been calculated for a variety of unsteady problems of interest to the helicopter community. Also acoustic intensities were calculated in a space fixed reference frame. As a result the propagation of acoustic waves due to blade-vortex interaction are better understood. It appears that both the changing lift and changing drag play a role in this propagation. When certain conditions exist the propagation is enhanced, while other conditions may inhibit this propagation, at least in certain directions. Computational fluid dynamics can be used in helping to determine what mach number and airfoil shape combinations lead to large acoustic propagation and what combinations do not.

References

1. George, A. R., and Chang, S. B., "Noise due to Transonic Blade-Vortex Interactions," Paper A-83-39-50-D000, 39th Annual National Forum of the American Helicopter Society, May 1983.

2. Wu, J. C., Sankar, N. L., and Hsu, T. M., "Unsteady Aerodynamics of an Airfoil Encountering a Passing Vortex," AIAA Paper 85-0203, Reno, Nev., 1985.

3. Jones, H. E., "The Aerodynamic Interaction between an Airfoil and a Vortex in Transonic Flow," Paper presented at the Workshop on Blade-Vortex Interactions (unpublished), Moffet Field, Calif., Oct. 1984.

4. Srinivasan, G. R., McCroskey, W. J., and Baeder, J. D., "Aerodynamics of Two-Dimensional Blade-Vortex Interaction," AIAA Paper 85-1560, Cincinatti, Ohio, 1985.

5. Ballhaus, W. F., and Goorjian, P. M., "Implicit Finite-Difference Computations of Unsteady Transonic Flows about Airfoils," AIAA Journal, Vol. 15, No. 12, Dec. 1977, pp. 1728-1735.

6. McCroskey, W. J., and Goorjian, P. M., "Interactions of Airfoils with Gusts and Concentrated Vortices in Unsteady Transonic Flow," AIAA Paper 83-1691, Danvers, Massachusettes, 1983.

7. Boxwell, D. A., and Schmitz, F. II., "Full-Scale Measurement of Blade-Vortex Interaction Noise," Journal of American Helicopter Society, Vol. 27, No. 4, Oct. 1982.

8. Tijdeman, H., and Seebass, R., "Transonic Flow Past Oscillating Airfoils," Annual Review of Fluid Mechanics, Vol. 12, 1980, pp. 181-222.
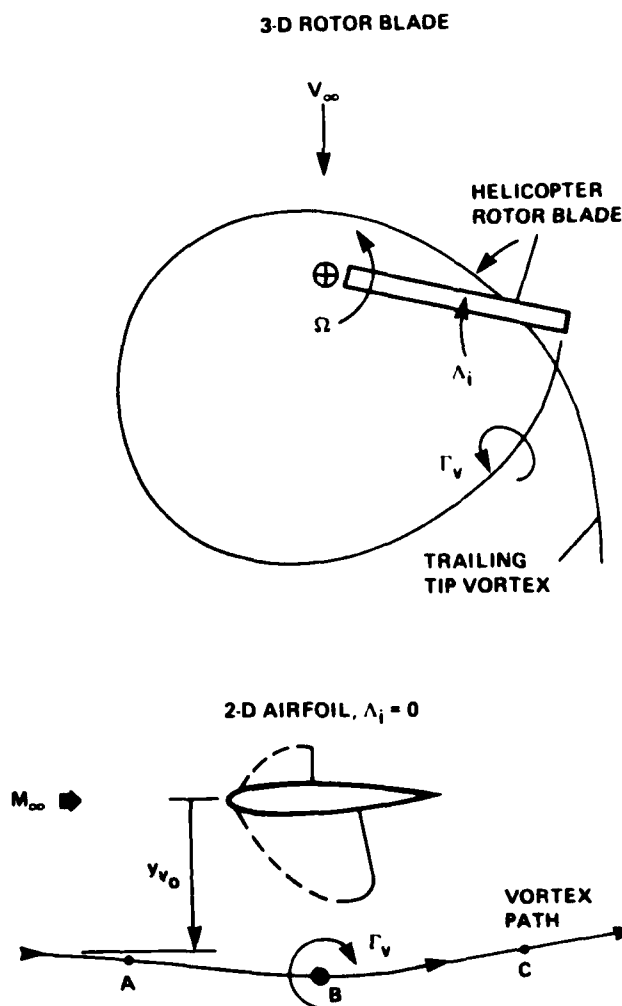
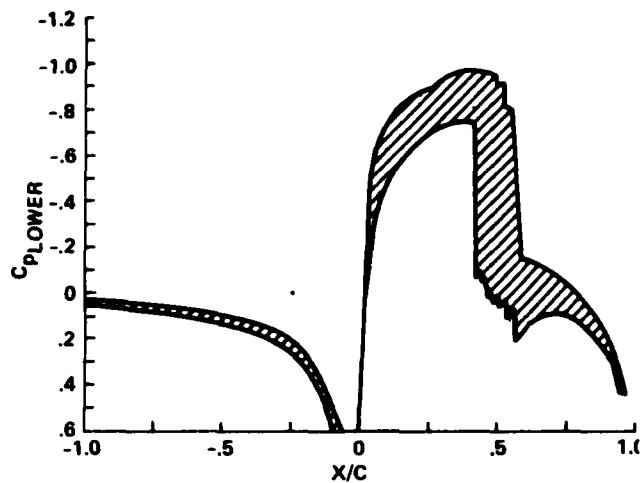Figure 1. Unsteady Vortex Interactions

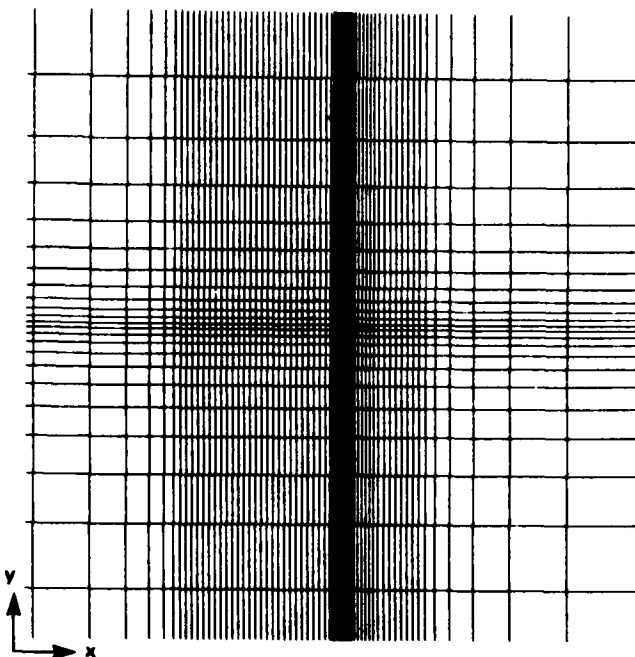Figure 2. Fluctuating Pressure Along Axis - NACA0012 Airfoil, $M_\infty = .80, y_v = -0.26, \Gamma_v = 0.20$
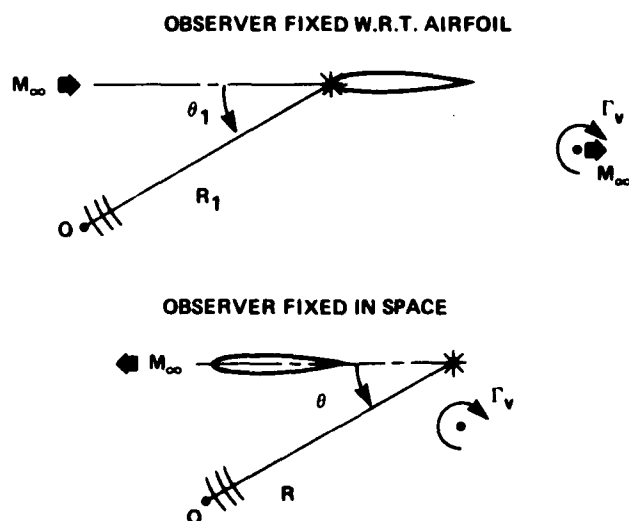

Figure 3. Computational Grid (Every Fifth Line Shown)

OBSERVER FIXED W.R.T. AIRFOIL

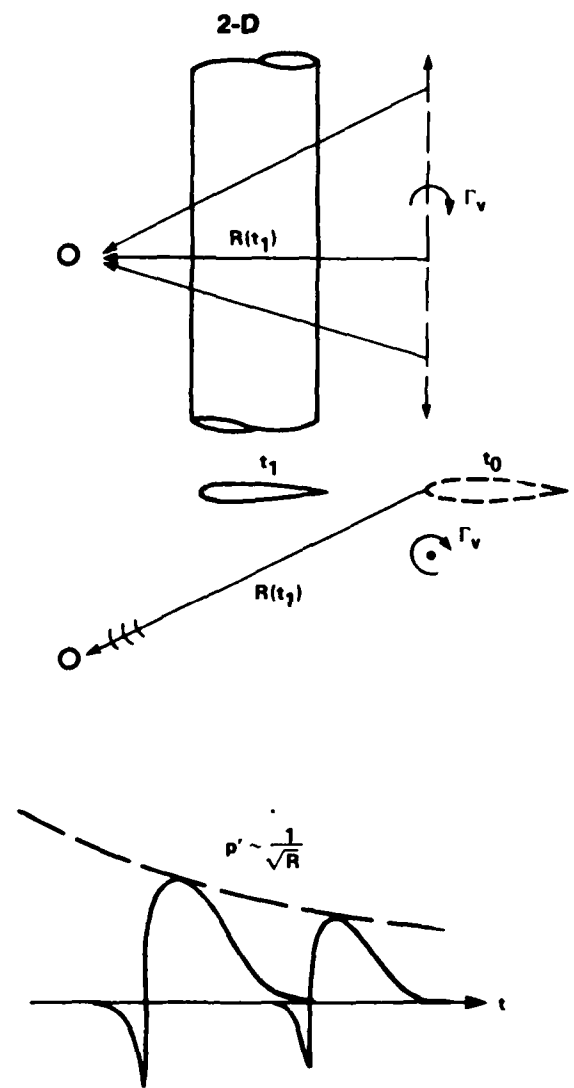**OBSERVER FIXED IN SPACE**

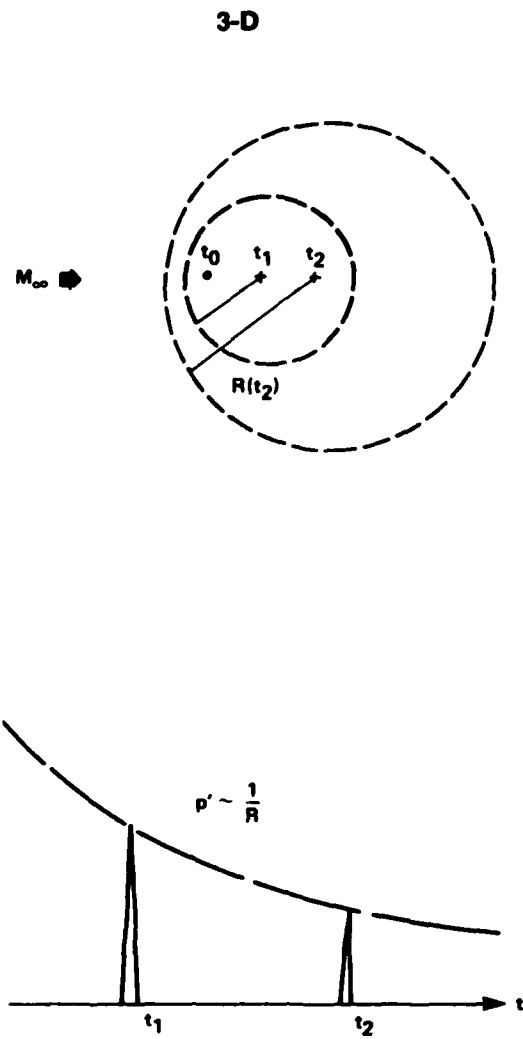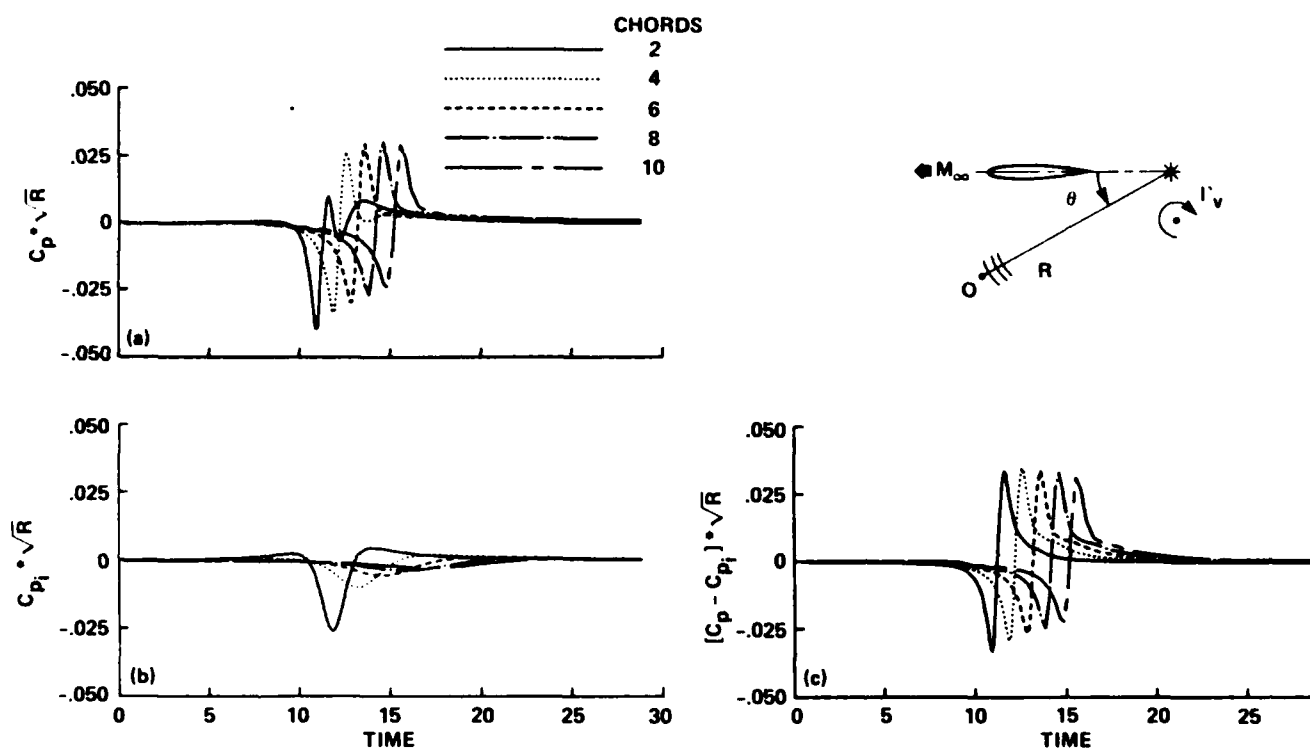Figure 4. Frames of Reference

Figure 5. Acoustic Theory

7

Figure 6. Pressure Time Histories
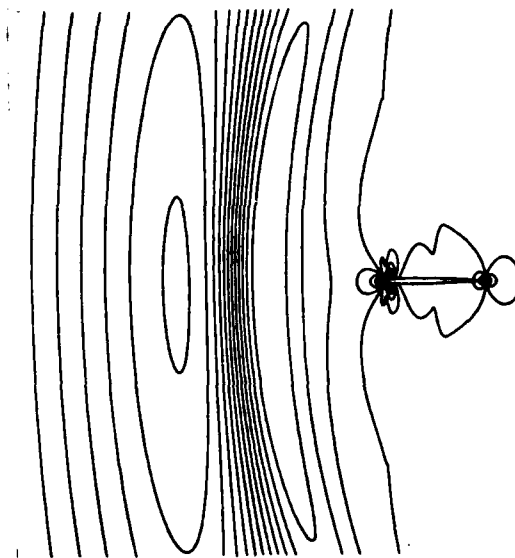NACA0012 Airfoil, 45 Degree Ray, $M_\infty = .50, y_v = -0.26, \Gamma_y = 0.20$

8

Figure 7. Thickenning-Thinning Airfoil
NACA0012 Airfoil, $M_\infty = .80$, Thickness = 6 - 12 - 6 %
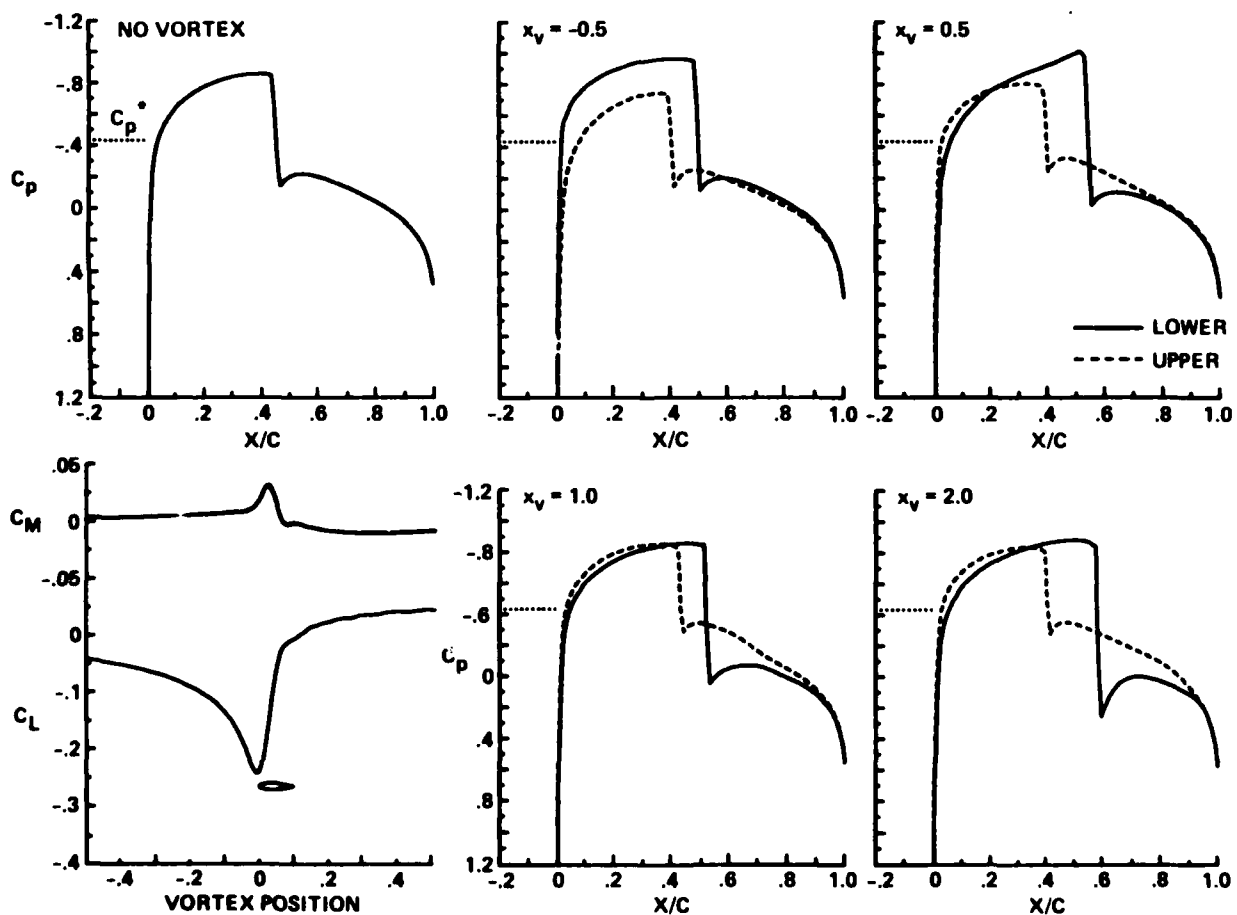
Figure 8. Surface Pressure and Cl and Cm Histories
NACA0012 Airfoil, $M_\infty = .80, y_v = -0.26, \Gamma_v = 0.20$

9
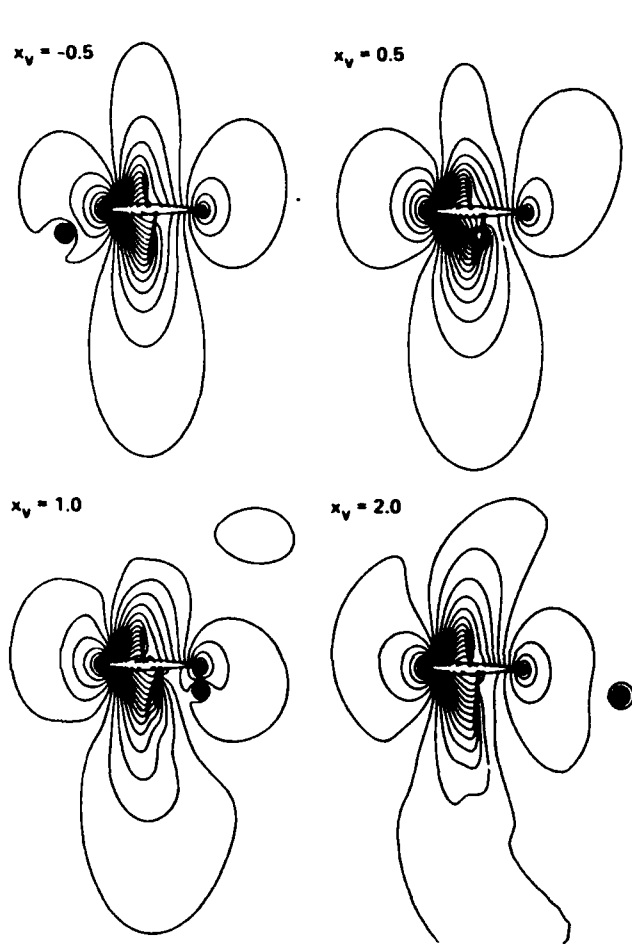
Figure 9. Pressure Contours - C_p
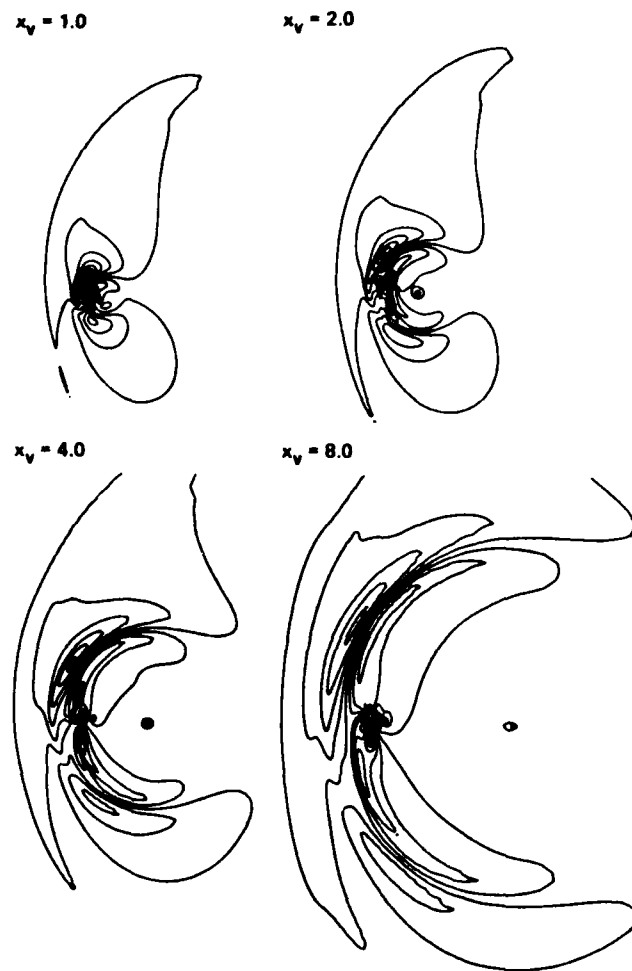NACA0012 Airfoil, $M_\infty = .80, y_v = -0.26, \Gamma_v = 0.20$

Figure 10. Disturbance Pressure Contours -
$(C_p - C_{p_s}) * Sqrt(R)$
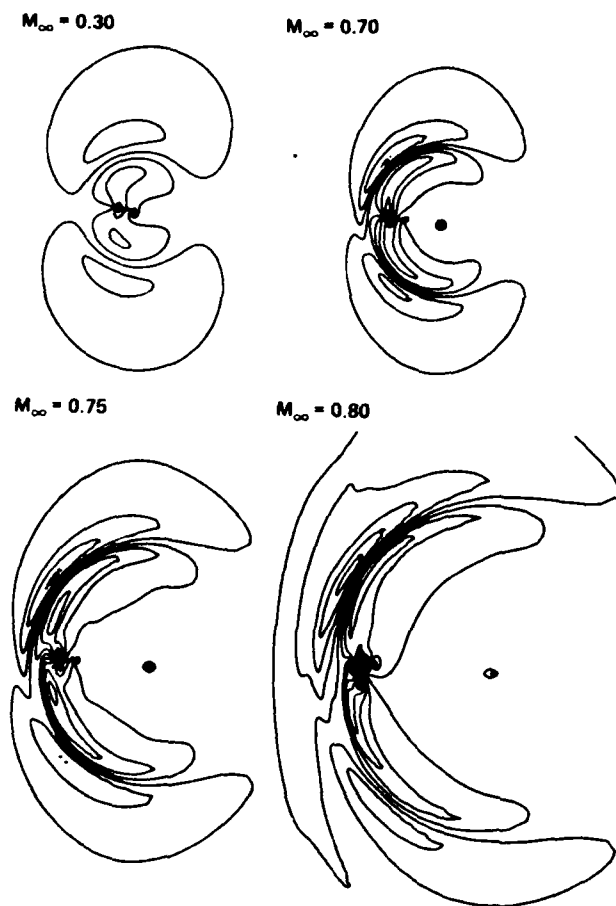NACA0012 Airfoil, $M_\infty = .80, y_v = -0.26, \Gamma_v = 0.20$

$M_\infty = 0.30$ $M_\infty = 0.70$

$M_\infty = 0.75$ $M_\infty = 0.80$

Figure 11. Disturbance Pressure Contours -
$(C_p - C_{p_s}) * Sqrt(R)$
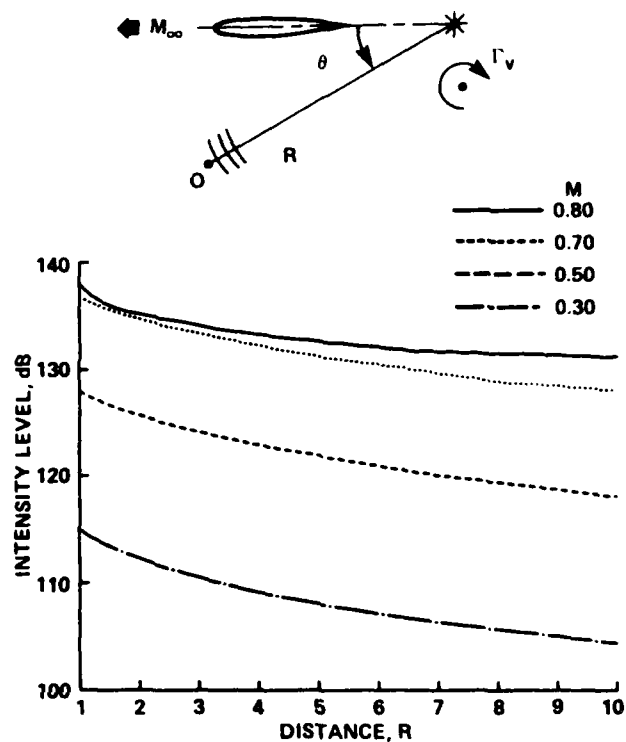NACA0012 Airfoil, $y_v = -0.26, \Gamma_v = 0.20$

Figure 12. Acoustic Intensity Versus Distance
NACA0012 Airfoil, 45 Degree Ray
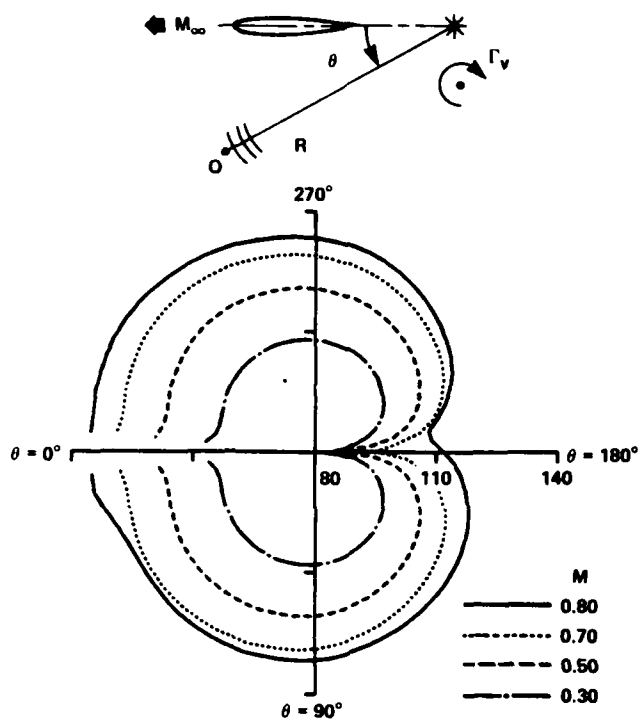$y_v = -0.26, \Gamma_y = 0.20$

11

Figure 13. Polar Plot of Acoustic Intensity
NACA0012 Airfoil, 10 Chord Arc
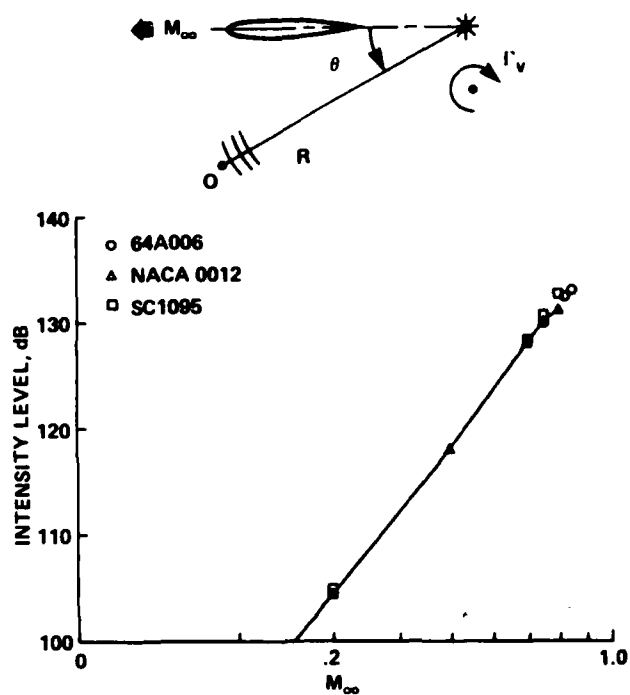$y_v = -0.26, \Gamma_y = 0.20$

Figure 14. Intensity Level Versus Mach Number
45 Degree Ray at 10 Chords
$y_v = -0.26, \Gamma_v = 0.20$

END

10-8-86

DTIC